

# Temperature dependence of carrier migration in ridge-shaped quantum-wire laser structures

Shinichi Watanabe<sup>A</sup>, Shyun Koshiba<sup>B</sup>, Masahiro Yoshita<sup>A</sup>,  
Motoyoshi Baba<sup>A</sup>, Hiroyuki Sakaki<sup>C</sup>, and  
Hidefumi Akiyama<sup>A</sup>

*A) Institute for Solid States Physics (ISSP), University of Tokyo,  
5-1-5 Kashiwa-no-ha, Kashiwa, 277-8581 Chiba, Japan*

*B) Faculty of Engineering, Kagawa University, 4-6-1 Saiwaityou, Takamatsu,  
Kagawa 760-8526, Japan*

*C) Institute of Industrial Science (IIS), University of Tokyo,  
7-22-1 Roppongi, Minato-ku, 106-8558 Tokyo, Japan*

*tel: +81-471-36-3387, fax: +81-471-36-3388, e-mail: shinchan@issp.u-tokyo.ac.jp*

The uniformity and the temperature dependence of carrier migration in the ridge-shaped quantum-wire (QWR) laser structures are studied by the micro- and macro-photoluminescence measurements. The structural inhomogeneity of the ridge structures is negligible in the optical wavelength scale of  $\sim \mu\text{m}$ , while it exists in the scale of  $\sim \text{nm}$  to perturb the electronic states of the active regions in the structures. Below  $T = 40 \text{ K}$ , the loss inherent to the carrier migration is not so large, however above  $T = 40 \text{ K}$ , the larger carrier diffusion length cause the carriers in the QWR region to flow away due to the structural inhomogeneity, and thus cause the higher threshold pump power for lasing.

After the theoretical predictions by Arakawa and Sakaki[1], low dimensional semiconductor laser structures have been the great interests to achieve the lower threshold current and less temperature dependence than the bulk semiconductor lasers. For the one-dimensional (1D) quantum wire (QWR) laser structures, Kapon *et al.* firstly reported the stimulated emission from the V-groove QWR laser structures[2]. Wegscheider *et al.* reported the lasing from the ground state exciton using the T-shaped QWR structures[3], and we reported the stimulated emission from the higher subbands in ridge-shaped QWR laser structures[4, 5]. Recently, stimulated emission from the one-dimensional ground subband in V-groove QWR is also reported[6, 7].

Although there are many methods to fabricate the QWR laser structures, the improvement of the temperature dependence has not been achieved yet. One of the reasons is the difficulty to uniformly form the QWR structures along the waveguide structure with about 1-mm of the cavity length. The structural inhomogeneity of QWRs derives the migration of photo-excited carriers into positions with local energy minimum, and the threshold current depends largely on temperature.

In this article, we first summarize our previous works [4, 5, 8] to distinguish the origins of photoluminescence (PL) and lasing in a ridge-shaped QWR laser structure, and after that, we discuss the uniformity of the QWR and the temperature dependence of carrier migration.

Figure 1 shows a cross-sectional transmission electron microscope (TEM) image of a ridge QWR laser structure. Separately confined-heterostructure (SCH) layers were formed. The core layer of the SCH was composed of a GaAs active layer with a nominal vertical thickness of 5 nm sandwiched by 90 nm thick barrier layers of a  $\text{Al}_{0.2}\text{Ga}_{0.8}\text{As}$  digital alloy. As a result, the QWR is formed at the ridge corner of the two adjacent QWs (side-QWs). The core layer was sandwiched by the cladding layers of the  $\text{Al}_{0.4}\text{Ga}_{0.6}\text{As}$  digital alloy to construct SCH optical waveguides[9]. The sample was cleaved to form optical cavities of length  $L = 300 \mu\text{m}$ . As shown in Fig. 1, we define the  $x$ -axis as the wire direction, the  $y$ -axis as the lateral confinement direction, and the  $z$ -axis as the growth direction.

Figure 2 shows the emission spectra of the ridge QWR at various excitation power from 10 mW to 100 mW ( $T = 4.7 \text{ K}$ ). The micro-PL imaging characterizations are performed to identify the position and pattern of emission at each spectral peak.

At 10 mW of pump power, two spectral peaks are assigned to (a)QWR (1.623 eV), (b)Side-QW (1.704 eV) individually by their emission images. At 100 mW of pump power, lasing is occurred at 1.666 eV of photon energy. The threshold carrier density is estimated to be  $\sim 4 \times 10^7 \text{ carriers/cm} \cdot \text{pulse}$  within the side-QWs

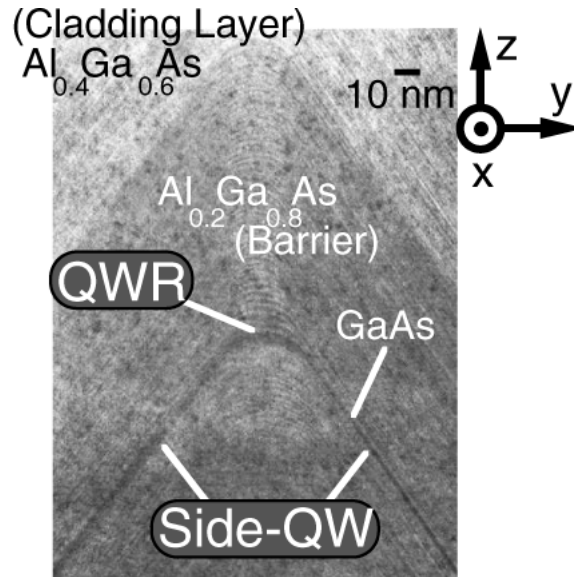


Fig. 1. Cross-sectional transmission electron microscope (TEM) image of a ridge QWR laser structure. The GaAs/ $\text{Al}_{0.2}\text{Ga}_{0.8}\text{As}$  QWR is formed at the ridge corner formed by two adjacent quantum wells (side-QWs). The  $x$ ,  $y$ , and  $z$  directions are defined as the wire direction ( $x$ ), the lateral confinement direction ( $y$ ), and the growth direction ( $z$ ).

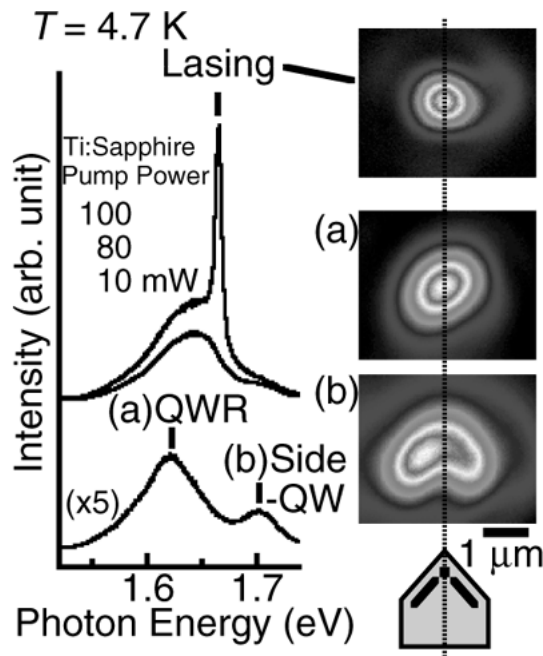


Fig. 2. (Left) Photoluminescence (PL) spectra from ridge QWR at 10, 80, 100 mW of excitation pump power ( $T = 4.7$  K). Lasing is occurred at 100 mW of pump power, 1.666 eV. (Right) Spectrally and spatially resolved cross-sectional contour-plot images (4.7 K) of emission corresponding to the two spectral peaks in the emission spectrum for 10 mW of pump power. Each spectral peak is assigned as QWRs (1.623 eV), side-QWs (1.704 eV) by its emission pattern. Image of lasing is also shown at the top for 100 mW of pump power. Note that the lasing image is centered at the top of ridge structure, similarly to the emission image of QWRs.

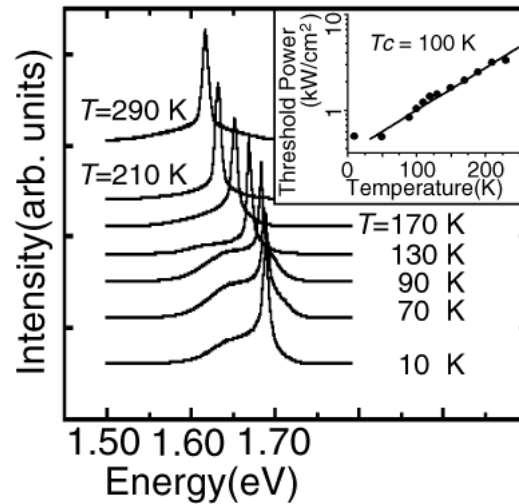


Fig. 3. Temperature dependence of stimulated emission spectrum from 10 K to 290 K. Spectral peak shift of lasing energy is mainly caused by that of band-gap energy with temperature. The inset shows temperature dependence of threshold pump power for stimulated emission, from which the characteristic temperature is estimated to be 100 K as the slope of semi-log plot.

and the QWR regions[5]. The lasing energy is blue-shifted from emission of the ground state of ridge QWRs by about 43 meV, while it is red-shifted from the emission of side-QWs by 38 meV. So the origin of lasing is most likely the transitions between higher-order excited states in QWRs.

Lasing image at 1.666 eV (100 mW) is shown at the top of the emission images. It is clearly recognized that the lasing image is centered at the top of ridge structure, similarly to the emission pattern of QWR. This is a very good assistance for our conclusion about the lasing mechanism that the lasing is due to transitions between higher-order excited states.

Temperature-dependent stimulated-emission measurements were also performed. Figure 3 shows spectrum of stimulated emission at each temperature. Optical excitation was performed by the green pulse laser (526 nm, 50 ps) in this measurement, so that we also excite the barrier  $\text{Al}_{0.2}\text{Ga}_{0.8}\text{As}$  region. Lasing was observed at all the temperatures between 4.7 K and 290 K. The lasing energy became gradually lower for higher temperatures. The change in the lasing energy was mainly caused by that of band-gap energy with temperature, so that the origin of the lasing was considered unchanged. The temperature dependence of threshold pump power for stimulated emission is also shown in the inset of Fig. 3, from which the characteristic temperature was estimated to be 100 K as the slope of semi-log plot.

The values of the threshold excitation power were rather large especially at high temperatures. One of the reasons is the substantial amount of loss occurring in the initial carrier capture process. A large portion of initially generated carriers in barrier layers undergoes surface recombination or other decay processes before they are captured in QWRs.

Another reason is broadened density of states (DOS) at the band edge due to the structural inhomogeneity of QWRs. In the regime where electrons and holes are saturated in their states, DOS limits gain.

To investigate the structural inhomogeneity of QWRs, we present spectrally- and spatially-resolved top-view PL imaging measurements under lasing and pre-lasing conditions. Contour-plot images in Fig. 4 show the top-view PL intensity mapping in the  $xy$  plane for a ridge laser structure at (a) 1.638 eV (QWR) and (b) 1.713 eV (side-QWs) of the two PL peak energies under pre-lasing condition (excitation power of  $0.07 \text{ kW/cm}^2$ ) at  $T = 4.7 \text{ K}$ . Figure 4(c) shows the top-view PL intensity mapping at 1.688 eV of the lasing photon energy under the lasing condition ( $1.6 \text{ kW/cm}^2$ ) at the same temperature. Uniform optical excitation by  $\text{Ti:Al}_2\text{O}_3$  laser pulses (1.777 eV of the photon energy) was performed from the top of the ridge structure, and PL and

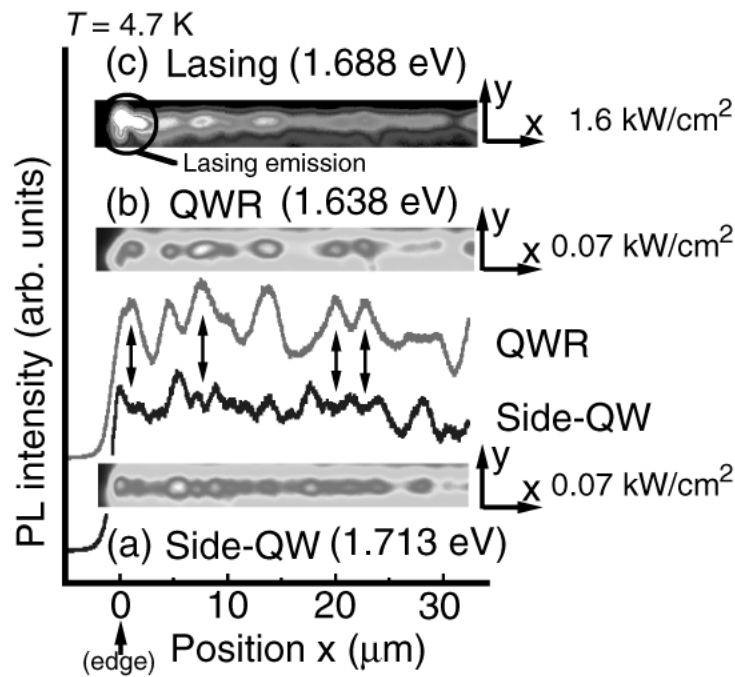


Fig. 4. (a), (b) Top-view PL intensity mapping in the  $xy$  plane for a ridge laser structure at two PL peak energies, 1.638 eV (QWR) and 1.713 eV (side-QW) with a band width of 2 nm, at  $T = 4.7$  K. Uniform optical excitation by Ti:Al<sub>2</sub>O<sub>3</sub> laser pulses (photon energy of 1.777 eV, excitation power of 0.07 kW/cm<sup>2</sup>) was performed from the top of the ridge structure, and PL from the top surface was collected via an objective lens and an interference filter. The ridge structure is along the  $x$  direction with its cleaved edge defined as  $x=0$ . The PL intensity profiles along the  $x$  axis for the QWR and the side-QWs are shown by the top and bottom lines, respectively. (c) Top-view PL intensity mapping at 1.688 eV of the lasing photon energy under the lasing condition (1.6 kW/cm<sup>2</sup>) at  $T = 4.7$  K.

lasing from the top surface was collected via an objective lens and an interference filter.

The  $x$ ,  $y$ , and  $z$  directions are the same as those defined in Fig. 1. The ridge wire structure is formed along the  $x$  direction with its cleaved edge defined as  $x=0$ . The images of the two adjacent side-QWs are not separated in Fig. 4(a) due to the spatial resolution of 1  $\mu\text{m}$  of the experimental setup[10]. The PL intensity profiles along the  $x$  axis for the (a)side-QWs and (b)QWR are shown by the top and bottom lines, respectively.

Strong stimulated emission signal was observed at the cleaved edge position ( $x=0$   $\mu\text{m}$ ) in Fig. 4(c). Although the lasing occurs in the ridge waveguide direction, the output light emitted from the cleaved edge diverges. Therefore the large numerical aperture collection optics makes it possible to observe stimulated emission even in the top-view configuration.

The every PL intensity profile showed an inhomogeneous PL pattern in Fig. 4, which indicates that the fluctuation of vertical thickness toward the  $z$  direction exists in the nanometer scale to perturb the quantized electronic states of the active region in the structure.

It should be noted that the inhomogeneity of the PL pattern is in a 2 ~ 3  $\mu\text{m}$  scale for the QWR along the  $x$  direction, whereas that for the side-QWs is in a 1  $\mu\text{m}$  scale, which is comparable to the spatial resolution of the measurement. The PL inhomogeneity results from the migration of photo-excited carriers into positions with local energy minimum. Thus, the 2 ~ 3  $\mu\text{m}$ -scale inhomogeneity indicates that the carriers are able to move along the QWR over a similar distance. We expect carrier diffusion in side-QWs along the wire direction to be inefficient, because the vertical thickness of side-QWs is thin, as is shown in Fig. 1.

Carrier migration from the side-QWs toward the QWR was also observed in the PL intensity profile in Fig. 4. At the positions indicated by arrows in Fig. 4, the intensity of the QWR is strong while that of the side-QWs is weak. This suggests that excited carriers in the side-QWs flow efficiently into the QWR at these positions, whereas at other positions with less carrier flows, more excited carriers recombine in the side-QW regions.

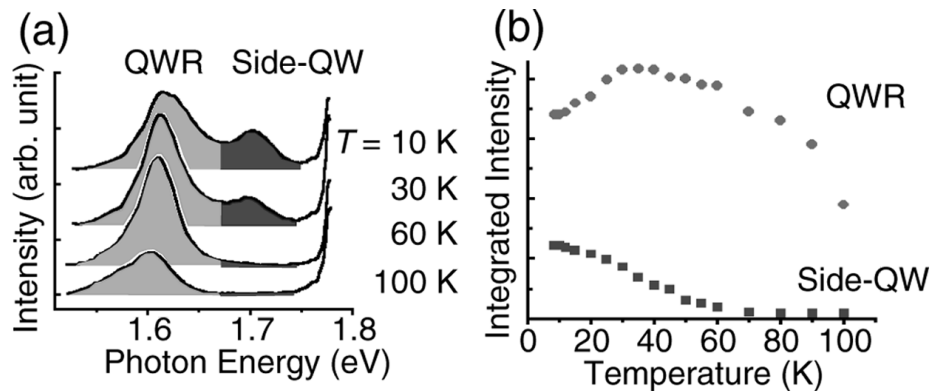


Fig. 5. (a) Temperature dependence of the macroscopic PL of the ridge QWR laser structures under weakly excitation. (b) Temperature dependence of the integrated PL intensity corresponding to the emission from QWR and side-QWs.

At the positions where PL of both QWR and side-QWs are weak, it is interpreted that emission occurred at lower energy with local energy minimum state or carriers recombined via nonradiative decay processes.

Note the top-view spontaneous emission profile at the lasing energy observed in Fig. 4 (c) is almost the same as that of the ground states of QWR emission profiles observed in Fig. 4 (b). Therefore, the origin of stimulated emission can be again safely assigned as the excited states of the QWR.

It should be noted that there is no scattered stimulated emission on the ridge waveguide structure ( $x > 0$   $\mu\text{m}$ ) in Fig. 4(c). This means that there are no significant scatterers in the ridge waveguide structure which cause scattering of light in the cavity and hence cause optical losses. Therefore, the structural inhomogeneity of the ridge structures is negligible in the optical wavelength scale of  $\sim \mu\text{m}$ , while it exists in the scale of  $\sim \text{nm}$  to perturb the electronic states of the active regions in the structures.

The fluctuations of vertical thickness cause the structural inhomogeneity along the QWR, which largely influences the migration of the photo-excited carriers inside the ridge structure. We next investigate the temperature dependence of carrier migration inside the ridge QWR structure.

Figure 5(a) shows the temperature dependence of the macroscopic PL of the ridge QWR laser structures under weakly excitation by cw-Ti:Al<sub>2</sub>O<sub>3</sub> laser (1 mW, 1.774 eV). Figure 5(b) shows the temperature dependence of the integrated PL intensity corresponding to the emission from QWR and side-QWs obtained from Fig. 5(a).

The PL intensity from the QWRs got larger, while that from the side-QWs got smaller as temperature increases below  $T = 40$  K. The total PL intensity from the QWR and the side-QWs was not been changed below  $T = 40$  K. Above  $T = 40$  K, both PL intensity got smaller as temperature increases.

The higher temperature causes the larger diffusion length of photo-excited carriers. Below  $T = 40$  K, the larger carrier diffusion length causes the photo-excited carriers generated in the side-QWs to efficiently migrate to the QWR region, so that the PL from the QWR gets stronger. The loss inherent to the carrier migration from side-QWs to the QWR is not so large, since the total PL intensity was not changed.

Above  $T = 40$  K, however the larger carrier diffusion length cause the carriers in the QWR region to flow into the local energy minimum state with lower transition energies, or flow into the defects which cause the non-radiative recombination of carriers. Therefore, the total PL intensity gets smaller.

Since the optical gain is limited by DOS proportional to the PL intensity, the threshold pump power for lasing also gets larger. To improve the uniformity of the QWRs is the very important subject in the future to improve the temperature dependence of the threshold pump power, and also to achieve ground subband lasing in QWRs.

In summary, the uniformity of the ridge-shaped QWR structures and the temperature dependence of carrier migration were studied by the PL measurements. Below  $T = 40$  K, the loss inherent to the carrier migration from side-QWs to the QWR is not so large. However above  $T = 40$  K, the larger carrier diffusion length cause the carriers in the QWR region to flow away due to the structural inhomogeneity, and thus cause the higher threshold pump power for lasing.

This work was partly supported by a Grant-in-Aid from the Ministry of Education, Science, Sports, and Culture, Japan. One of the authors (S. W.) would like to thank JSPS for the partial financial support.

## References

1. Y. Arakawa and H. Sakaki, Appl. Phys. Lett. **40**, 939 (1982).
2. E. Kapon, D. M. Hwang, and R. Bhat, Phys. Rev. Lett. **63**, 430 (1989).
3. W. Wegscheider, L. N. Pfeiffer, M. M. Dignam, A. Pinczuk, K. W. West, S. L. McCall, and R. Hull, Phys. Rev. Lett. **71**, 4071 (1993).
4. S. Watanabe, S. Koshiba, M. Yoshita, H. Sakaki, M. Baba, and H. Akiyama, Appl. Phys. Lett. **73**, 511 (1998).
5. S. Watanabe, S. Koshiba, M. Yoshita, H. Sakaki, M. Baba, and H. Akiyama, Appl. Phys. Lett. **75**, 2190 (1999).
6. T. G. Kim, X. L. Wang, R. Kaji, and M. Ogura, Physica E **7**, 508 (2000).
7. L. Sirigu, D. Y. Oberli, L. Degiorgi, A. Rudra, and E. Kapon, Physica E **7**, 513 (2000); Phys. Rev. B **61**, 10575 (2000).
8. S. Watanabe, M. Yoshita, M. Baba, H. Akiyama, S. Koshiba, and H. Sakaki, Technical Digest. Summaries of papers presented at the *Quantum Electronics and Laser Science Conference*, QTuF3, pp. 60 (1999).
9. S. Koshiba, S. Watanabe Y. Nakamura, M. Yamauchi, M. Yoshita, M. Baba, H. Akiyama, and H. Sakaki, J. Crystal Growth **201/202**,810(1999).
10. M. Yoshita, H. Akiyama, T. Someya, and H. Sakaki, J. Appl. Phys. **83**, 3777 (1998).